

On Dirac sheet configurations of $SU(2)$ lattice fields

E.-M. Ilgenfritz^a, B. V. Martemyanov^b, M. Müller-Preussker^a
 and A. I. Veselov^b

^a Humboldt-Universität zu Berlin, Institut für Physik, D-10115 Berlin, Germany

^b Institute for Theoretical and Experimental Physics, Moscow 117259, Russia

November 21, 2018

Abstract

Finite temperature Euclidean $SU(2)$ lattice gauge fields close to the deconfinement phase transition are subjected to cooling. We find relatively stable or absolutely stable configurations with an action below the one-instanton action $S_{inst} = 2\pi^2$ both in the deconfinement and the confinement phases. In this paper we attempt an interpretation of these lowest action configurations. Their action is purely magnetic and amounts to $S/S_{inst} \approx N_t/N_s$, where N_t (N_s) is the timelike (space-like) lattice size, while the topological charge vanishes. In the confined phase part of the corresponding lattice configurations turns out to be absolutely stable with respect to the cooling process in which case Abelian projection reveals a homogeneous, purely Abelian magnetic field closed over the "boundary" in one of the spatial directions. Referring to the dyonic structure established for the confinement phase near T_c and based on the observation made for this phase that such events below the instanton action S_{inst} emerge from dyon-antidyon annihilation, the question of stability (metastability) is discussed for both phases. The hypothetically different dyonic structure of the deconfinement phase, inaccessible by cooling, could explain the metastability.

1 Introduction

In the confined phase, below but sufficiently close to T_c , applying cooling to Monte Carlo generated $SU(2)$ lattice gauge fields has shown a dyonic structure of metastable action plateaus [1, 2, 3, 4]. The dyons themselves correspond, in a good approximation, to the constituents of Kraan-van Baal-Lee-Lu (KvBLL) caloron solutions [5, 6, 7]. The same cooling applied to lattice configurations in the deconfined phase acts entirely differently.

There is no remnant dyonic structure. Instead of this, there are metastable events on some lowest action plateau (actually significantly below the one-instanton action $S_{inst} = 2\pi^2$). These configurations have vanishing topological density, and the action is purely magnetic. Such configurations have been already observed and discussed many years ago in papers by Laursen and Schierholz [8], and Veselov and Polikarpov [9].

In the present paper, from the perspective gained with the dyonic structure at high enough temperature, we try to give a new interpretation of the lowest action configurations seen in Refs. [8, 9]. For this goal we study them both in confined and deconfined phases. In the confinement phase we are in the fortunate position that we can observe the parent configurations which sometimes evolve into the configurations considered here. In all observed cases this parent configuration was a dyon-antidyon pair. Contrary to this, in the deconfined phase the cooling technique has been unable to exhibit potential parent configurations in the form of action plateaus, i.e. approximate solutions of the lattice equations of motion (metastable plateaus of action). We have critically examined the 't Hooft-Polyakov monopole structure of the cooled configurations emerging from the deconfinement phase that was suggested in Ref. [8]. We do confirm to see a minor fraction of magnetic configurations which resemble 't Hooft-Polyakov monopoles at a first view. However, even for these rare events we find only a weak correlation between the localization of magnetic action and the positions of monopoles defined either in terms of the Polyakov line or of the magnetic charge in the Weyl gauge.

On the contrary, the similarity of the action dependence for these configurations on the spatial size of the lattice suggestively points toward their common nature. Most likely, in both cases we would expect quantized magnetic fluxes. The returned flux (unavoidable in the maximal Abelian projection for periodic boundary conditions and manifesting itself as a Dirac string) can be visualized as Dirac sheet (swept out by a Dirac string moving in Euclidean time). Hence, we adopt the name Dirac Sheets (DS) for this class of observed cooled lattice configurations. DS configurations are known as exact solutions of the lattice field equations in $U(1)$ LGT [10].

The paper is organized as follows.

In Section 2 we will provide all necessary lattice definitions, in particular the observables considered in order to identify KvB and DS solutions.

In Section 3 we report on the statistics and the properties of DS events observed both in the confined and the deconfined phases.

Section 4 contains our conclusions.

2 Production and characterization of DS solutions

Throughout this paper $SU(2)$ gauge theory in four-dimensional Euclidean space is considered on an asymmetric lattice with periodic boundary conditions in all four directions. The respective ensembles of configurations have been created by heat bath Monte Carlo

using the standard Wilson plaquette action

$$S = \sum_{\vec{x}, t} s(\vec{x}, t) = \sum_{\vec{x}, t} \sum_{\mu < \nu} s(\vec{x}, t; \mu, \nu), \quad (1)$$

$$s(\vec{x}, t; \mu, \nu) = \beta \left(1 - \frac{1}{2} \text{tr} U_{x, \mu\nu} \right), \quad U_{x, \mu\nu} = U_{x, \mu} U_{x+\hat{\mu}, \nu} U_{x+\hat{\nu}, \mu}^\dagger U_{x, \nu}^\dagger$$

with inverse coupling $\beta = 4/g_0^2$. For simplicity the lattice spacing is set equal to $a = 1$. The lattice size was $N_s^3 \times N_t$ with the spatial extension $N_s = 8, 10, 12, 16, 20$ and with the inverse physical temperature $T^{-1} \equiv N_t = 4$. For $N_t = 4$ the model is known to undergo the deconfinement phase transition at the critical coupling $\beta_c \simeq 2.299$ [11]. Throughout this paper we will use two ensembles with $\beta = 2.2 < \beta_c$ and $\beta = 2.4 > \beta_c$.

The equilibrium field configurations in both ensembles have been cooled by iterative minimization of the Wilson action S . In one or another form, cooling is used in order to smooth out short-range fluctuations, while (initially) leaving untouched some large-scale properties of the configurations. The cooling method applied here is the standard relaxation method described long time ago in [12] and was used for investigation of instantons [12, 13].

This method, if applied without any further limitation, easily finds approximate solutions of the lattice field equations as shoulders (plateaus) of the action as a function of cooling steps (relaxation history). Here we shall concentrate on smoothed fields at the very last stages of cooling, using a stopping criterium which selects the plateaus in the interval of action $S \leq 0.6 S_{\text{inst}}$.

The emerging gauge field configurations were analyzed according to the spatial distributions of the following observables:

- *action density* computed from the local plaquette values:

$$s(\vec{x}, t) = \sum_{\mu < \nu} s(\vec{x}, t; \mu, \nu), \quad (2)$$

(see eq.(1));

- *topological density* computed with the standard twisted plaquette discretization:

$$q_t(\vec{x}) = -\frac{1}{2^4 \cdot 32\pi^2} \sum_{\mu, \nu, \rho, \sigma = \pm 1}^{\pm 4} \epsilon_{\mu\nu\rho\sigma} \text{tr} [U_{x, \mu\nu} U_{x, \rho\sigma}]; \quad (3)$$

- *Polyakov loop* defined as:

$$L(\vec{x}) = \frac{1}{2} \text{tr} P \quad (4)$$

with

$$P(\vec{x}) = \prod_{t=1}^{N_t} U_{\vec{x}, t, 4}, \quad (5)$$

where the $U_{\vec{x}, t, 4}$ represent the links in time direction;

- *non-stationarity* defined as:

$$\delta_t = \sum_{\vec{x}, t} |s(\vec{x}, t+1) - s(\vec{x}, t)| / S ; \quad (6)$$

- *violation of equations of motion* Δ

$$\Delta = \frac{1}{4N_s^3 N_t} \sum_{x, \mu} \frac{1}{2} \text{tr} [(U_{x, \mu} - \bar{U}_{x, \mu})(U_{x, \mu} - \bar{U}_{x, \mu})^\dagger] , \quad (7)$$

where

$$\bar{U}_{x, \mu} = c \sum_{\nu \neq \mu} \left[U_{x, \nu} U_{x+\hat{\nu}, \mu} U_{x+\hat{\mu}, \nu}^\dagger + U_{x-\hat{\nu}, \nu}^\dagger U_{x-\hat{\nu}, \mu} U_{x+\hat{\mu}-\hat{\nu}, \nu} \right] \quad (8)$$

is the local link x, μ being the solution of the lattice equation of motion, with all degrees of freedom coupled to it held fixed. The factor c is just a normalization of the staple sum such that $\bar{U}_{x, \mu} \in SU(2)$ ¹.

- *Abelian magnetic fluxes and monopole charges* defined within the Weyl (or generalized temporal) gauge, $\partial_0 A_0 = 0$, and the maximally Abelian gauge (MAG). The first one is obtained from the Polyakov gauge (PolG, achieved by diagonalizing $P(x)$ in each lattice site, followed by Abelian gauge transformations which render the (then diagonal) temporal links $U_{\vec{x}, \tau; 4}$ independent on time τ . The latter is found by maximizing the gauge functional A

$$A[g] = \frac{1}{2} \sum_{x, \mu} \text{tr}(U_{x, \mu}^g \tau_3 U_{x, \mu}^{g^\dagger} \tau_3) , \quad (9)$$

under gauge transformations $U_{x, \mu} \rightarrow U_{x, \mu}^g = g(x) U_{x, \mu} g^\dagger(x + \hat{\mu})$. The abelianicity is the maximum value of this quantity divided by the number of links.

In both cases, Abelian link angles $\theta_{x, \mu}$ are then defined by Abelian projection onto the diagonal $U(1)$ part of the link variables $U_{x, \mu} \in SU(2)$. According to the DeGrand-Toussaint prescription [14] a gauge invariant magnetic flux $\bar{\Theta}_p$ through an oriented plaquette $p \equiv (x, \mu\nu)$ is defined by splitting the plaquette $\Theta_p = \theta_{x, \mu} + \theta_{x+\hat{\mu}, \nu} - \theta_{x+\hat{\nu}, \mu} - \theta_{x, \nu}$ into $\Theta_p = \bar{\Theta}_p + 2\pi n_p$, $n_p = 0, \pm 1, \pm 2$ such that $\bar{\Theta}_p \in (-\pi, +\pi]$. The magnetic charge of an elementary 3-cube c is then $m_c = \frac{1}{2\pi} \sum_{p \in \partial c} \bar{\Theta}_p$.

For the cooling procedure of equilibrium gauge field configurations we have kept the standard periodic boundary conditions on the $4D$ torus.

Finally, cooling was stopped at some (n -th) cooling iteration step when the following criteria for the action S_n were simultaneously fulfilled:

- $S_n < 0.6 S_{\text{inst}}$,

¹The replacement $U_{x, \mu} \rightarrow \bar{U}_{x, \mu}$ is exactly the local cooling step as applied throughout this paper.

- $S_n - 2 S_{n-1} + S_{n-2} < 0$.

The last condition means that the relaxation just passed a point of inflection. As we have empirically observed, the point of inflection always coincides, within an accuracy of plus/minus one global cooling step, with a minimal violation of the equations of motion Δ . This can be understood as follows. If violation of equations of motion $\Delta = 0$, i.e. equations of motion are fulfilled we are in the local minimum of the action where its variation is zero. If violation of equations of motion Δ has the minimum the variation of the action has also the minimum and second variation of the action is zero what means that the action goes through the point of inflection.

3 Properties of Dirac Sheets in the confined and the deconfined phases

3.1 Cooling

We have investigated DS events on lattices $N_s^3 \times N_t$ with $N_t = 4$ and $N_s = 8, 10, 12, 16, 20$. The statistics and the mean actions of various types of configurations selected by the cooling process are presented in Table 1 and Figures 1 and 2 where the dependence of \bar{S}/S_{inst} on N_s/N_t and N_t/N_s is shown to have the tendency $S_{DS}/S_{inst} \rightarrow N_t/N_s$. Their properties are summarized in Table 2 and illustrated by the remaining Figures. We have found DS becoming very stable at action values $\simeq S_{inst} \cdot N_t/N_s$. The (color-)electric contribution to the total action is very small compared with the magnetic contribution. Moreover, they are perfectly static with the values of nonstaticities δ_t shown in Table 2. Employing MAG we have convinced ourselves that they are almost Abelian (see the abelianicity A in Table 2), and only a small fraction contains MAG monopoles.

In the confinement phase it happens quite rarely that they appear *directly* in the result of the cooling process. In all cases observed they appear after dyon-antidyon pairs have been observed at $S \approx S_{inst}$ which annihilate in the final stage of relaxation. The Abelian monopole content of DS in the deconfinement phase, if it is obtained by Abelian projection in the Weyl gauge, amounts to monopole-antimonopole pairs being present in 60 ÷ 90% of those cooled configurations.

We originally had found this type of solution for fixed holonomy boundary conditions (f.h.b.c.) [1, 2, 3, 4]. These DS for f.h.b.c. were seen to be oriented very exactly in plane and to have non-zero action for plaquettes in one of the space-space coordinate planes (x, y) , (x, z) or (y, z) . They had the same action values S/S_{inst} as we have found later on for the case of periodic boundary conditions. We had also found configurations which contained two DS orthogonal to each other at action values twice as large than for one DS. We shall not further comment on such events in this paper.

Table 1: The statistics of DS events on the lattices $N_s^3 \times N_t$ with $N_s = 8, 10, 12, 16, 20$ for $\beta = 2.20$ (confined phase, upper row) and $\beta = 2.40$ (deconfined phase, lower row). \bar{S} denotes the average action of the observed events, δS the variance.

β	N_s/N_t	N_{event}	S/S_{inst}	$\delta S/S_{inst}$
2.2	2.0	33	0.479	0.007
2.4	2.0	54	0.471	0.004
2.2	2.5	18	0.392	0.009
2.4	2.5	62	0.387	0.003
2.2	3.0	12	0.331	0.002
2.4	3.0	73	0.323	0.002
2.2	4.0	11	0.249	0.0007
2.4	4.0	66	0.245	0.002
2.2	5.0	7	0.200	0.000
2.4	5.0	28	0.195	0.002

3.2 Can DS configurations be viewed as 't Hooft-Polyakov monopoles in the deconfinement phase ?

In contrast to previous parlance (these configurations have been called "monopole" (M) configurations in Refs. [8, 3]) we have called them here Dirac Sheet (DS) configurations from the beginning. Now we want to provide some more facts supporting this interpretation. In the beginning let us recall several features which originally suggested the interpretation as 't Hooft-Polyakov monopoles.

There should be

- a minimum of the dynamically generated "Higgs field" $\text{tr}(A_0/T)^2$
- a maximum of the (almost purely) magnetic action density $\text{tr}B^2$
- a pair of pointlike Abelian magnetic charges, one carrying action and the other being spurious.

We have studied these signatures for our configurations cooled down below the one-instanton level starting from the deconfinement phase, *i.e.* from equilibrium Monte Carlo configurations on a $16^3 \times 4$ lattice at $\beta = 2.4$. All these configurations have one maximum of the magnetic action and a relatively shallow maximum of the Polyakov line. A subset of these configurations, considered in the Weyl or maximally Abelian gauge, respectively, has a pair of corresponding static magnetic charges. The relative frequencies actually to find the indicated Abelian monopole structure is given in Table 2.

Table 2: The properties of DS events on the lattices $N_s^3 \times N_t$ with $N_t = 4$, $N_s = 8, 10, 12, 16, 20$. For each N_s the events are presented in three rows: unstable (upper row) and absolutely stable (middle row) DS in the confined phase for $\beta = 2.20$ and DS in deconfined phase for $\beta = 2.40$ (lower row).

N_s/N_t	frequency of DS events	fraction of DS with monopoles in Weyl gauge	fraction of DS with monopoles in MAG	A	Δ	δ_t
2.0	3.8%	21.1%	5.3%	98.8%	0.223E-05	0.372E-03
2.0	3.2%	-	-	100%	0.944E-09	0.253E-06
2.0	4.4%	59.1%	6.8%	98.0%	0.355E-05	0.889E-03
2.5	3.0%	41.7%	8.3%	98.9%	0.122E-05	0.426E-03
2.5	4.8%	-	-	100%	0.167E-15	0.245E-12
2.5	11.3%	79.4%	2.9%	98.8%	0.107E-05	0.512E-03
3.0	2.0%	50.0%	-	99.5%	0.378E-06	0.214E-03
3.0	5.7%	-	-	100%	0.150E-15	0.389E-12
3.0	14.3%	88.4%	-	99.1%	0.464E-06	0.397E-03
4.0	0.3%	-	-	99.9%	0.385E-10	0.103E-07
4.0	5.0%	-	-	100%	0.760E-15	0.108E-10
4.0	16.0%	72.9%	14.6%	99.5%	0.665E-07	0.149E-03
5.0	-	-	-	-	-	-
5.0	2.8%	-	-	100%	0.636E-16	0.245E-11
5.0	18.0%	77.8%	11.1%	99.7%	0.244E-07	0.951E-04

One of the cooled configurations with a Weyl gauge monopole pair is portrayed in Figure 3 where we show the profiles of action density and Polyakov line over the (x, z) plane which cuts the configuration and contains the maximum of action density. In Figure 4 the positions of the static monopole pair are projected onto that (x, z) plane. This event indeed shows a structure as reported in Ref. [8].

For a more quantitative assessment, we have compared the positions of the maxima of three-dimensional action density and the Polyakov loop. We found the average distance equal to 7 ± 2 lattice spacings, whereas for the maximum of the action density and the position of the nearest Weyl gauge magnetic monopole the distances are somewhat less, 5.2 ± 1.6 lattice spacings. These distances are certainly smaller than the maximal three-dimensional distance $8\sqrt{3} \approx 13$ but are difficult to reconcile with a static extended particle (monopole) interpretation.

Monopoles obtained in the MAG are present only in approximately $< 15\%$ of all DS events (see also Table 2). One of the rare cases when a DS event in the deconfinement phase shows an Abelian monopole-antimonopole pair in MAG is presented in Figs.5 and

6.

3.3 More on the Dirac sheet interpretation

At this point it might be useful to focus on the striking volume dependence of the action (common to both phases) and on the surprising stability of the cooled DS configurations (which distinguishes the confinement phase) in order to understand similarities and differences between the ways how these configurations originate from the respective vacuum of the two phases.

The dependence of \bar{S}/S_{inst} on N_s/N_t and N_t/N_s is shown on Figures 1 and 2. In the confined phase for $N_s = 20$ all 7 DS events were absolutely stable with $S_{DS}/S_{inst} = N_t/N_s$. The number N_t/N_s can be understood as follows. Let there be a quantized homogeneous Abelian magnetic flux in some spatial (x , y or z) direction. The Abelian magnetic field is equal to $B_x^3 = 4\pi/N_s^2$. Its action is equal to [10]

$$S_{DS} = \frac{4}{g_0^2} (1 - \cos(\frac{B_x^3}{2})) N_s^3 N_t \approx \frac{1}{2g_0^2} (B_x^3)^2 N_s^3 N_t = \frac{8\pi^2}{g_0^2} \frac{N_t}{N_s} = S_{inst} \frac{N_t}{N_s}. \quad (10)$$

All 7 DS events in the confined phase for $N_s = 20$ (when put into MAG) show such an Abelian magnetic field. There arises the question: why for other (smaller) N_s in the confined phase the fluxes are not always homogeneous and absolutely stable, and why the fluxes are unstable for all N_s in the deconfined phase. The probable answer is that magnetic flux (during the process of $D\bar{D}$ annihilation) is not always closed over the "boundary" in some periodic spatial direction. If the size of dyons in the $D\bar{D}$ pair is small compared to the spatial size of the lattice, the annihilation is almost pointlike and the magnetic flux has a good chance to be closed.

The size distribution of dyons depends on holonomy. In the confined phase the measure of holonomy $L = \cos(2\pi\omega)$ (ω being the holonomy parameter) is distributed in the neighbourhood of zero. For lower plateaus of action the distribution approaches more and more the semicircle law (Haar measure). Then ω is distributed over the range $0 \leq \omega \leq 1/2$ and the size of the lighter dyon as known from the KvB solution ($N_t/4\pi\omega$ for $0 \leq \omega \leq 1/4$ and $N_t/4\pi(1/2 - \omega)$ for $1/4 \leq \omega \leq 1/2$ measured in lattice spacings) varies from N_t/π to the maximal value possible on the finite lattice. In the deconfined phase, the holonomy becomes closer and closer to the trivial one ($L \approx \pm 1$) and the dyons (in the dyon-antidyon pair) are strongly delocalized. As mentioned in the Introduction, during cooling in the deconfined phase the dyon-antidyon pair itself does not become visible on a well-established plateau.

The correlation between holonomy and stability of DS events is shown in Figure 7 for both phases. It can be understood if the configurations are really emerging from the annihilation of a dyon-antidyon pair. The Figure presents scatter plots where each DS event is represented by two points: (s_{min} , holonomy) and (s_{max} , holonomy) with s_{min} and s_{max} being the action density at sites where it is minimal and maximal, respectively). Provided that the holonomy remains far enough from trivial, we obtain DS events from the

confined phase which consist of homogeneous Abelian magnetic fluxes. The homogeneity is expressed by $s_{min} = s_{max}$ and corresponds to the successful annihilation of more or less pointlike dyon-antidyon pairs. However, for values of holonomy close to trivial holonomy DS events in both confined and deconfined phase occur as unstable magnetic fluxes which are not closed as the result of annihilation of less localized (and "massless", i. e. low-action) dyons. The unstable DS in confined and deconfined phases have similar characteristics as can be seen from the first and third rows (shown separately for each N_s) in Table 2.

So, unstable DS events in confined and deconfined phases are similar. There is no absolute gap between unstable and absolutely stable DS events in the confined phase. This can be an argument in favor of their common nature. The stable DS events found in the confined phase are purely Abelian magnetic fluxes.

4 Conclusions

We have generated $SU(2)$ lattice gauge fields at non-zero temperature, both in the confined and the deconfined phases. We have cooled them in order to analyze the structure of the lowest action plateau (which in fact is below the one-instanton action). We have found certain structures ("Dirac sheets") that resemble homogeneous Abelian magnetic fluxes. The action dependence on the spatial lattice size N_s favors such an interpretation. For the deconfinement phase, where an 't Hooft-Polyakov monopole interpretation has been advocated, the loose correlation between different possible definitions of how to localize the monopole as an extended heavy particle makes this picture less convincing. Instead, we have looked for another interpretation in terms of how the original dyonic structure (which is different in the two phases) becomes destroyed by the cooling process. In the infinite volume limit $N_s \rightarrow \infty$, these DS structures disappear. Therefore, we interpret them as artefacts of the finite lattice volume.

Acknowledgements

We gratefully acknowledge the kind hospitality of the Instituut-Lorentz of the Universiteit Leiden extended to three of us (E.-M.I., B.V.M. and M.M.-P.) and helpful discussions with Pierre van Baal and Falk Bruckmann when the revised version of this paper became completed. This work was partly supported by RFBR grants 04-02-16079, 03-02-16941 and 02-02-17308, by the INTAS grant 00-00111, the CRDF award RP1-2364-MO-02, DFG grant 436 RUS 113/739/0 and RFBR-DFG grant 03-02-04016, by Federal Program of the Russian Ministry of Industry, Science and Technology No 40.052.1.1.1112. One of us (B.V.M.) gratefully appreciates the support of Humboldt-University Berlin where this work was initiated.

References

- [1] E.-M. Ilgenfritz, M. Müller-Preussker, and A. I. Veselov, in: Proceedings of the NATO Advanced Research Workshop on Lattice Fermions and Structure of the Vacuum, Dubna, Russia, 5 - 9 October 1999, V. K. Mitrjushkin and G. Schierholz (Editors), NATO ASI Series C, Vol. 553, Kluwer Academic, Dordrecht, 2000, p. 345, e-Print Archive: hep-lat/0003025.
- [2] E.-M. Ilgenfritz, B. V. Martemyanov, M. Müller-Preussker, and A. I. Veselov, Nucl. Phys. Proc. Suppl. **94** (2001) 407.
- [3] E.-M. Ilgenfritz, B. V. Martemyanov, M. Müller-Preussker, and A. I. Veselov, Nucl. Phys. Proc. Suppl. **106&107** (2002) 589.
- [4] E.-M. Ilgenfritz, B. V. Martemyanov, M. Müller-Preussker, S. Shcheredin, and A. I. Veselov, Phys. Rev. **D66** (2002) 074503.
- [5] T. C. Kraan and P. van Baal, Phys. Lett. **B428** (1998) 268, Phys. Lett. **B435** (1998) 389.
- [6] T. C. Kraan and P. van Baal, Nucl. Phys. **B533** (1998) 627.
- [7] K. Lee and C. Lu, Phys. Rev. **D58** (1998) 1025011.
- [8] M. L. Laursen and G. Schierholz, Z. Phys. **C38** (1988) 501.
- [9] A.I. Veselov, M.I. Polikarpov, in: "Multiprocessor computer system ES-1037 - ES-2707: experiences in system development and in the numerical simulation of nonlinear physical problems", Moscow, Space Research Institute, pp. 133-138 (1987).
- [10] V. K. Mitrjushkin, Phys. Lett. **B389** (1996) 713.
- [11] J. Engels, J. Fingberg, and V. K. Mitrjushkin, Phys. Lett. **B298** (1993) 154; J. Engels, S. Mashkevich, T. Scheideler, and G. Zinovev, Phys. Lett. **B365** (1996) 219.
- [12] E.-M. Ilgenfritz, M. L. Laursen, M. Müller-Preussker, G. Schierholz, and H. Schiller, Nucl. Phys. **B268** (1986) 693.
- [13] M.I. Polikarpov, A.I. Veselov, Nucl. Phys. **B297** (1988) 34.
- [14] T. A. DeGrand and D. Toussaint, Phys. Rev. **D22** (1980) 2478.

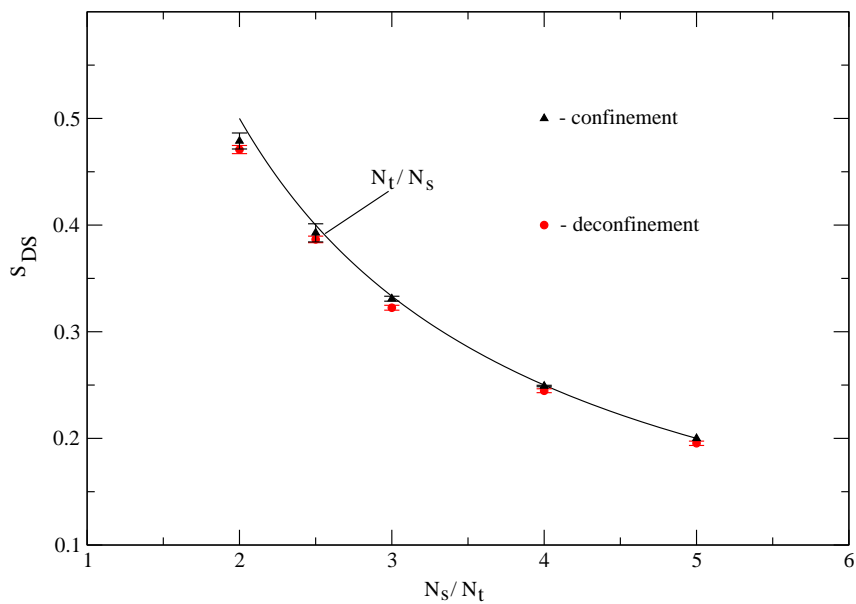


Figure 1: Action of DS events in the confined (triangles) and in the deconfined (circles) phases for lattices with $N_t = 4$ and $N_s = 8, 10, 12, 16, 20$ as function of N_s/N_t .

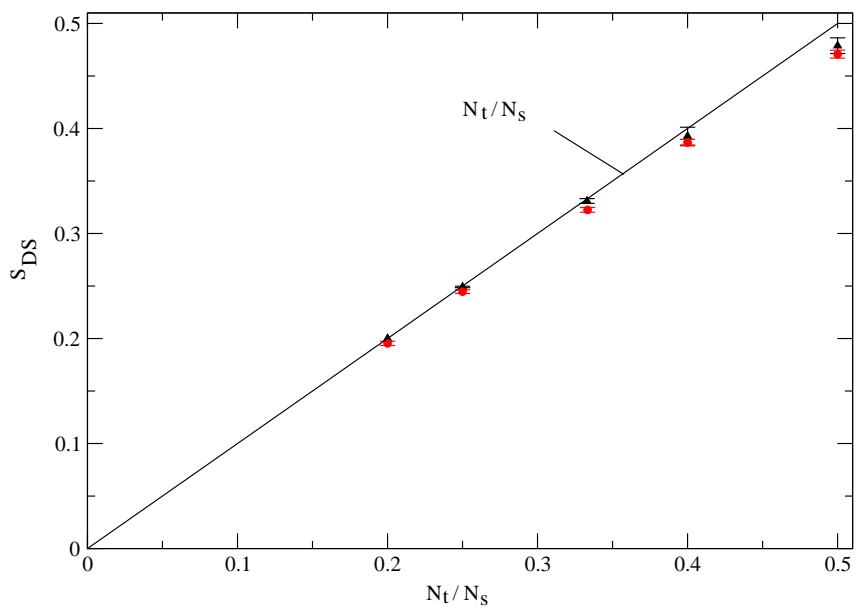


Figure 2: Same as in Fig. 1 as function of N_t/N_s .

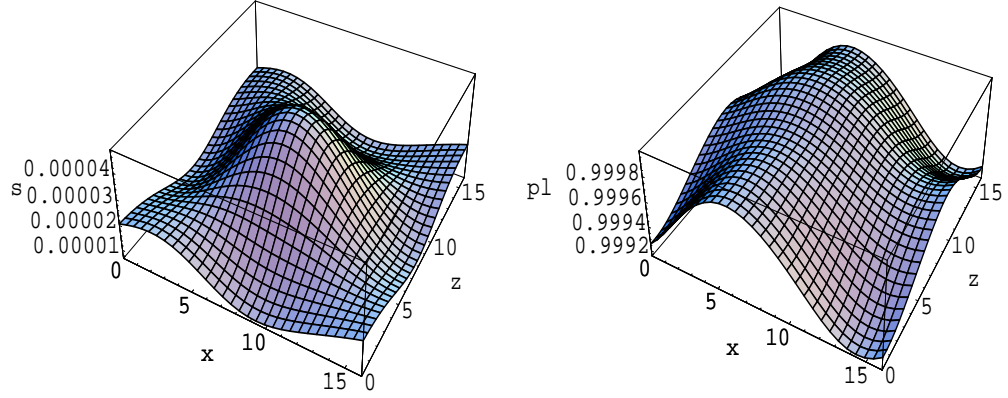


Figure 3: Action density (left) and Polyakov line (right) of an DS event in the deconfined phase shown as function over the xy plane cutting through the maximum of action density.

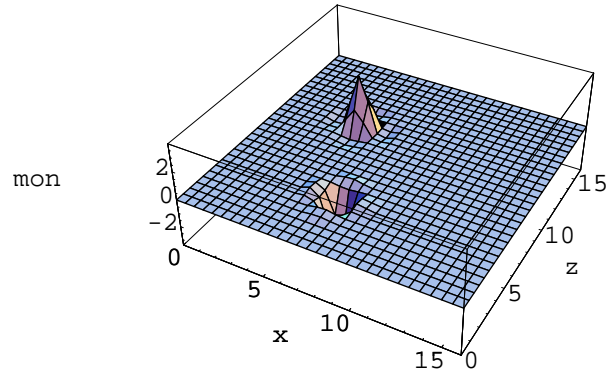


Figure 4: Abelian monopole charge density in Weyl gauge (summed over z) of the DS event presented on Fig.3. For static monopoles the monopole charge density is equal to $\pm N_t = \pm 4$. The smearing is due to the interpolation in MATHEMATICA graphics.

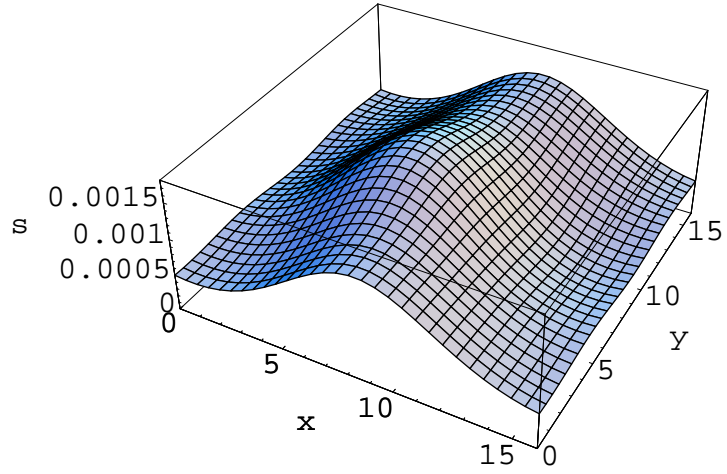


Figure 5: Action density (summed over t and z) of an DS event in the deconfined phase shown as function over the xy plane.

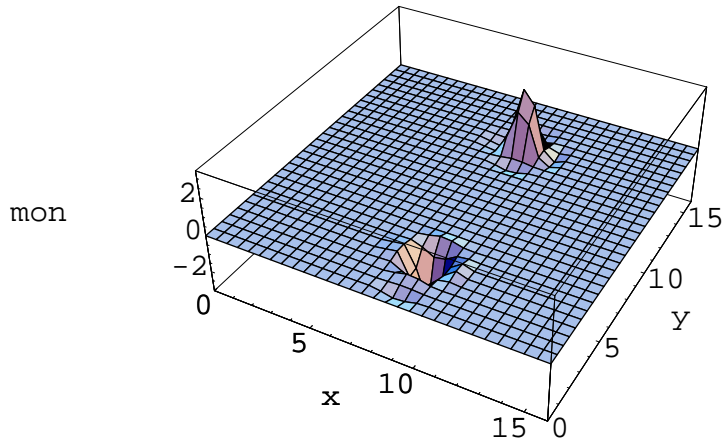


Figure 6: Abelian monopole charge density in MAG (summed over z) of the DS event presented on Fig.5. For static monopoles the monopole charge density is equal to $\pm N_t = \pm 4$. The smearing is due to the interpolation in MATHEMATICA graphics.

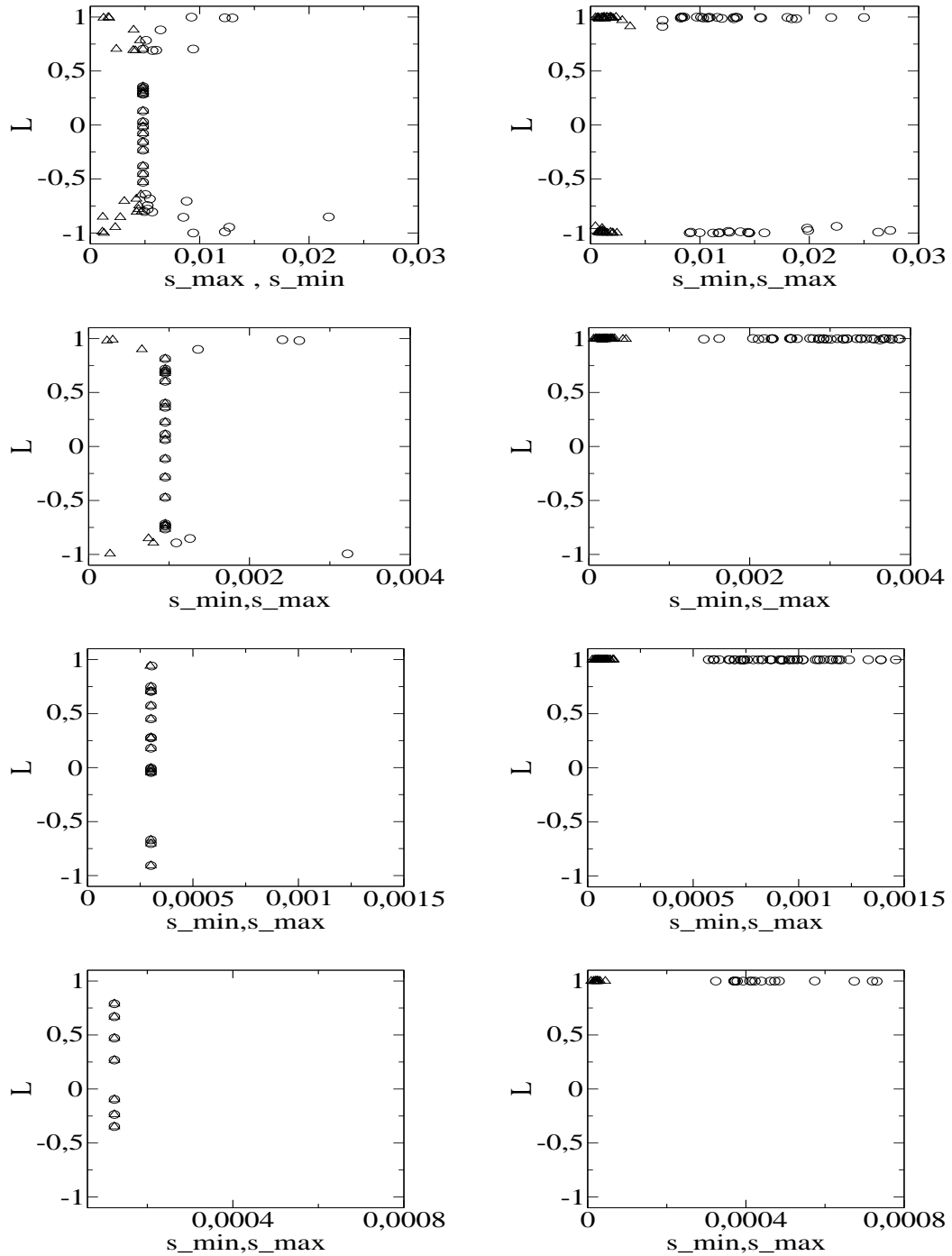


Figure 7: Correlation between the Polyakov loop L and the stability of DS configurations, illustrated by scatter plots showing, for each DS event, two points: (s_{min}, L) (as triangles) and (s_{max}, L) (as circles) with s_{min} (s_{max}) being the minimal (maximal) action density of the DS configuration. The left column presents DS events in the confined phase for lattices with $N_t = 4$ and $N_s = 8, 12, 16, 20$ (from up to down), the right column presents DS events in the deconfined phase for the same lattice sizes.